Section Characteristics of a Finite, Swept Circulation Control Airfoil

N. J. Wood*
Stanford University, Stanford, California

A three-dimensional wind-tunnel test of a circulation control wing has been performed. The data obtained indicated that the section characteristics for the wing may be approximated from two-dimensional data, even in the presence of wing sweep and finite span. No first-order effects of sweep were apparent in the degree of mixing between the trailing-edge jet and the upper surface boundary layer. The finite extent of the trailing-edge jet was shown to introduce additional contributions to the downwash distribution along the span in response to the vorticity shed at the jet extremities.

Nomenclature

A_n = coefficient in downwash equation
c = airfoil chord
C_ℓ = section lift coefficient
C_m = midchord pitching moment
c_p = pressure coefficient
c_p^* = pressure coefficient corresponding to locally sonic conditions
C_μ = blowing momentum coefficient
M_∞ = freestream Mach number
s = wing semispan
S = wing reference area
V,w = freestream and downwash velocities, respectively
x,y = chordwise and spanwise coordinates, respectively
α = angle of attack
η = nondimensional spanwise location, y/s
θ = angle in downwash equation, $\arccos(\eta)$
Λ = leading-edge sweep angle

Subscripts

u = unswept
s = swept

Introduction

A CIRCULATION control airfoil controls the location of the rear stagnation point on the bluff trailing edge as a function of the momentum injection of a thin wall jet located near the trailing edge.[1] These airfoils exhibit the unique capability of lift generation in the absence of changing angle of attack. The lift generation is a result of the addition of momentum into the upper surface boundary layer and the subsequent delay of flow separation, which in turn deflects the stagnation streamline further around the Coanda surface. At low speeds, lift coefficients of the order of 4 are readily achievable for modest blowing requirements, and the maximum lift augmentation $\partial C_\ell/\partial C_\mu$ of such devices is typically of the order of 60, nearly an order of magnitude higher than a conventional jet flap.

Recent two-dimensional experiments have provided researchers with an improved understanding of the parameters that affect the performance of these airfoils, a key parameter being the condition of the upper surface boundary layer as it approaches the jet exit. Effects due to Mach number, angle of attack, and Reynolds number, as well as the basic effects of airfoil thickness and camber, have all been correlated from examination of the boundary layer condition. The resulting performance trends have recently been summarized by Wood and Nielsen.[1]

A present application for circulation control airfoils is in the field of rotary wing and stopped rotor vehicles, where it is anticipated that the cyclic and collective blowing may replace mechanical cyclic and collective pitch. The performance benefits of such systems would enable significant improvements in the operational capabilities of VTOL aircraft. Such vehicles experience highly swept flow over the rotating blades, even to the 90-deg sweep case at high advance ratios. The purpose of the present study was therefore to examine the effects of three-dimensional flow, including sweep angle, on a circulation control wing and to show that two-dimensional data bases may be used for performance estimation of three-dimensional rotors. In particular, attention was given to the determination of whether the three-dimensional boundary layer on the upper surface of the wing affected the lift generation properties of these airfoils.

The addition of a blowing slot at the trailing edge of an airfoil introduces some complexity in an experiment solely to determine the effects of sweep on performance. Principally, the concept of an infinitely yawed wing, with different yaw angle capability, is not simple due to the varying length requirement for the blowing slot. As such, the present experiment considered a finite wing of high aspect ratio that could be rotated to different leading-edge sweep angles, both positive and negative. It was hoped that the data obtained could be used to examine the first-order effects of wing sweep if suitable allowances were made for the varying downwash distributions. The data reported will consider the results of experiments for the unswept and the 45-deg aft sweep cases and was acquired as a subset of a larger experimental program that included flow visualization.

Experimental Apparatus

A three-dimensional circulation control wing was designed and fabricated for testing in the NASA Ames 6×6-ft supersonic wind tunnel. A generic circulation control airfoil section based on a 20%-thick uncambered ellipse was chosen (Fig. 1). The section was fore-and-aft symmetric, and the leading- and trailing-edge contours were formed by the blending of circular arcs into the elliptic section, the radius of the circular arcs being approximately 4% of the airfoil chord. A single trailing-

Presented as Paper 86-1817 at the 4th Applied Aerodynamics Conference, San Diego, CA, June 2-4, 1986; received Aug. 14, 1986; revision received Sept. 17, 1986.

*Research Associate, Department of Aeronautics and Astronautics. Member AIAA.

edge blowing slot was incorporated into the trailing-edge geometry at the 96.3% chordwise location with a nominal slot height of 0.2% of the airfoil chord. The internal contours were carefully blended to ensure tangentiality of the exit flow and smoothness of the Coanda surface. The chord of the model was 10 in. and the aspect ratio approximately 8, based on the full span in the unswept configuration. For the 45-deg aft sweep configuration, the aspect ratio based on the full span reduced to 3.5. A body of revolution was used to remove the wing root from proximity to the wall boundary layer, and the body extended approximately one chord either side of the wing, depending on the sweep angle.

Static pressure taps were mounted at five spanwise stations, normal to the leading edge, which corresponded to 10, 30, 50, 70, and 90% of the unswept semispan. At each station, sufficient tappings were available to allow accurate calculation of the local section properties by integration. In addition, several spanwise and 45-deg inclined rows of taps were included to provide additional information. All the pressure taps were connected to a standard Scanivalve pressure-measuring system, which was controlled and sampled by an on-line data-acquisition system. This system also monitored the tunnel conditions and provided on-line graphical presentations. The jet blowing momentum was obtained from measurements of the mass flow of the jet m from an orifice plate and from estimation of the jet velocity V_j from the internal pressure by use of the isentropic flow equations.[1] The blowing momentum coefficient is

$$C_\mu = \frac{mV_j}{qS}$$

For the unswept case, a range of Mach numbers (0.3–0.5) and angles of attack (−5 to +5 deg) were each evaluated for a range of jet pressure ratios (1.0 to 3.0). For the swept case, the same range of blowing intensities was examined over a range of Mach numbers and angles of attack calculated to match the unswept case including the first-order effects of sweep.

$$\alpha_s = \alpha_u \cdot \cos\Lambda, \qquad C_{p_s} = \frac{C_{p_u}}{\cos^2\Lambda}, \qquad M_{\infty_s} = \frac{M_{\infty_u}}{\cos\Lambda}$$

For all experiments, the slot height was maintained at its original design value, and the effects of different Reynolds numbers were not investigated. In all cases, unless otherwise stated, the lift, pitching moment, and blowing momentum coefficients presented were calculated based on dynamic pressures normal to the leading edge of the wing.

Results and Discussion

This experiment had two primary objectives: first, to examine the effects of sweep on section characteristics within the limitations of a finite wing experiment and, second, to observe the effects of the finite wing on the spanwise load distribution and its response to blowing momentum. The effects of wing sweep on section lift performance are illustrated in Fig. 2 for the 70% spanwise station. This figure shows the lift obtained as a function of blowing momentum at zero incidence for a range of freestream Mach numbers. The unswept performance trends are as expected with reference to lift augmentation, maximum lift coefficient, and stall shape. The collapse of the swept (45-deg aft) and unswept data when corrected as conventional airfoils is well demonstrated. The comparison of the performance levels at any spanwise location is dependent on the three-dimensional effects of the finite wing and their variation with sweep angle. It will subsequently be demonstrated that this particular station, 70% span, was a location where the induced downwash angles were approximately equal for both the swept and unswept configurations. The apparent increase in the lift augmentation at the highest Mach number which is coupled with an improvement in the maximum lift

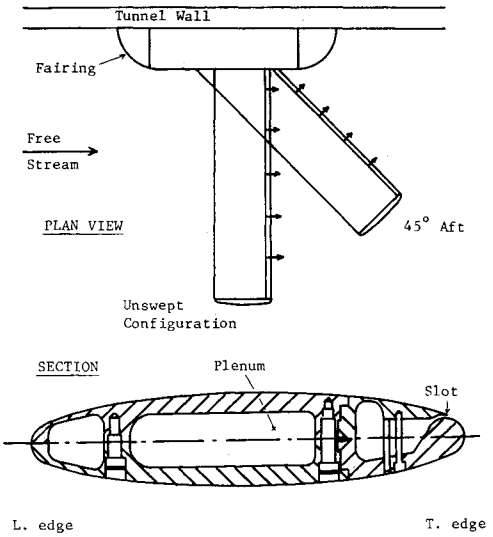

Fig. 1 Model geometry arrangement.

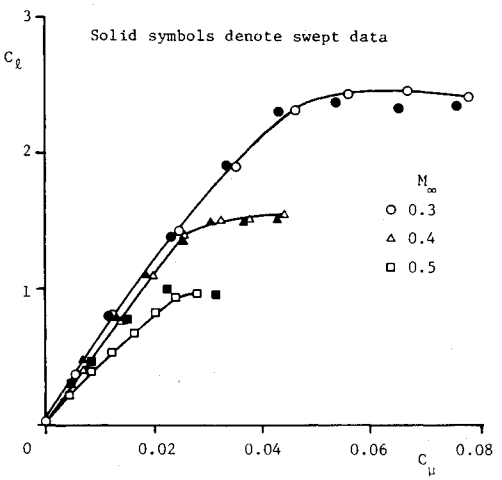

Fig. 2 Effect of wing sweep on section lift at $\alpha = 0$ deg, $\Lambda = 0$, 45 deg.

coefficient is a phenomenon yet to be explained. It was, however, observed to be a phenomenon that spread inboard from the tip as a function of increasing Mach number and was evidenced in the changing downwash distributions in the swept configuration.

Figures 3 and 4 show the effects of angle of attack for two different freestream Mach numbers for the 70% spanwise station. The superimposed data for the swept configuration have been corrected for both the Mach number normal to the leading edge as well as the angle of attack; for clarity, only a portion of the data is presented. Again, the comparison shows satisfactory first-order agreement between the two data sets and also exhibits the usually expected trends of decreasing lift augmentation with increasing angle of attack and regions of constant lift augmentation at negative angles of attack and low blowing coefficient.

The results from the flow visualization studies performed concurrently with the data acquisition revealed that the boundary layer approaching the slot reflected the presence of wing sweep.[2] A significant difference in the surface flow angles existed between the boundary layer and the jet, which exited normal to the slot lip at all times.[3] It was also apparent that this difference in flow angle reduced significantly toward the tip of the wing, indicating the strong three-dimensionality of the flowfield. These observations, coupled with the apparent collapse of the measured pressure data, provide strong evidence that there is little dependence of the mixing rate of

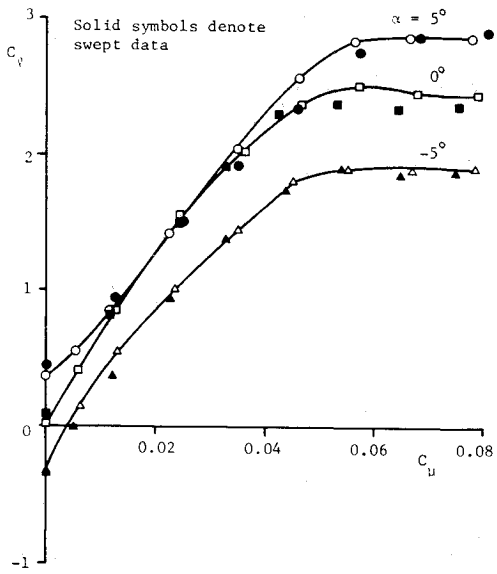

Fig. 3 Effect of angle of attack on lift at 70% span at $M_\infty = (0.3)_u$.

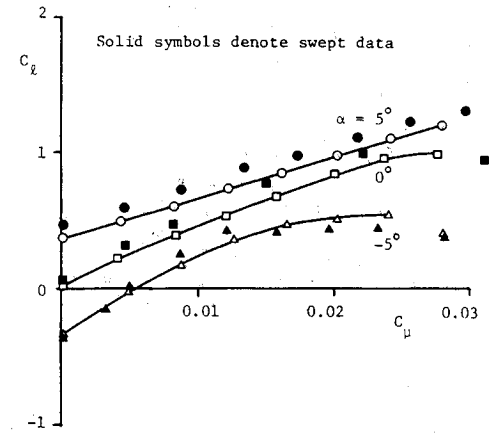

Fig. 4 Effect of angle of attack on lift at 70% span at $M_\infty = (0.5)_u$.

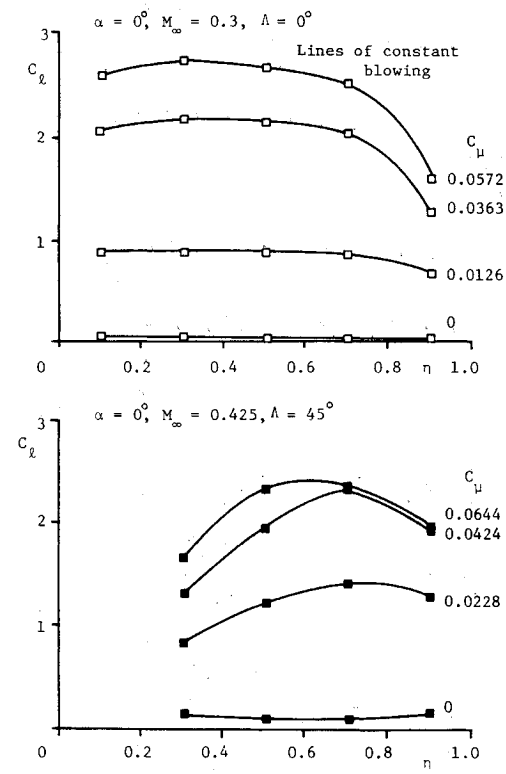

Fig. 5 Spanwise load distributions for the swept and unswept configurations.

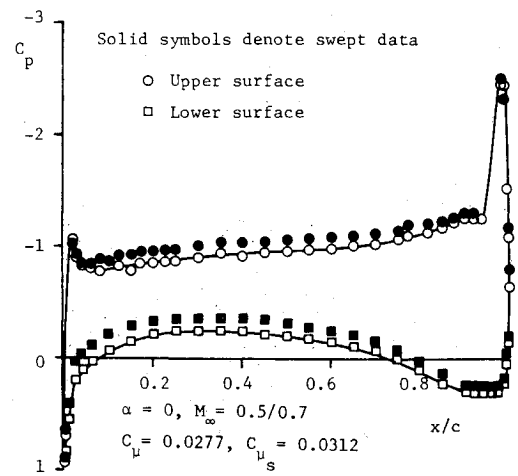

Fig. 6 Comparison of pressure distributions at the 70% spanwise location.

the jet and the freestream on the flow angle between them—at least at the 70% spanwise station where the initial comparisons were performed.

Evidence of a leading-edge separation bubble was also observed from oil flow visualization on the swept wing at angles of attack in excess of 5 deg. This is in direct correlation with the occurrence of alpha stall as seen from the lift coefficient results. The bubble was extremely small, less than 1% chord in extent and was positioned at the junction of the elliptic and circular arc contours, at approximately 3.5% chord. The bubble extended across the span and was presumably formed by a laminar separation followed by a turbulent reattachment. The location of the bubble is not surprising since, at the surface junction, extremely high rates of change of the second derivative of the surface curvature occur, resulting in sudden changes in the boundary-layer properties.

The spanwise loading exhibits significant variations as sweep is introduced. Figure 5 illustrates the change in the spanwise load distributions that were measured for the swept and unswept configurations. Unswept, it would appear that the circulation control wing produced a uniform load variation with blowing along the span with a tip lift loss appearing at approximately one chord from the tip. This uniform loading is not unexpected since the slot height was maintained at a constant value across the entire span. For the swept configuration, a strong skew in the loading is apparent, with a peak value at approximately 65% span. This asymmetry is also evidenced on conventional swept wings[4] and is due to the skewing of the bound vorticity at the root and tip of the wing. For the present experiment, this affect may have been aggravated by the presence of the relatively large body fairing.

Figures 6 and 7 show the comparison of the measured distributions at the 70 and 30% spanwise stations. These distributions exhibit the typical aft loading characteristic of circulation control airfoils due to the strong attachment and turning of the trailing-edge wall jet. The variation in the effective angles of attack for the two locations may be inferred from the differing suction peaks present at the leading edge of the airfoils since, for both cases, the blowing momentum was approximately equal. The inboard section exhibits a significantly more negative incidence when swept compared to the unswept case, while at the 70% span station, the angles are apparently almost equal. This illustrates an effect of sweep when coupled with a finite wing, i.e., the reduction of the downwash at the tip and the increase in the downwash at the root. The apparent increase in the trailing-edge suction peak toward the root of the wing may be due to the differences in

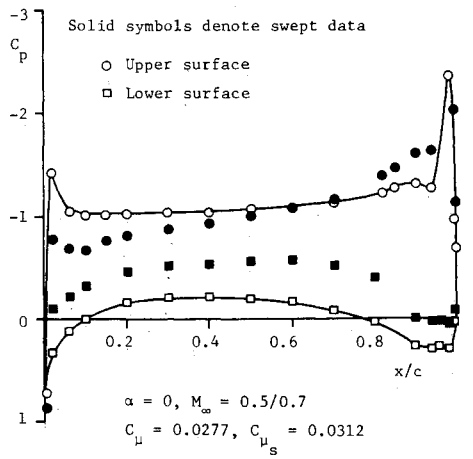

Fig. 7 Comparison of pressure distributions at the 30% spanwise location.

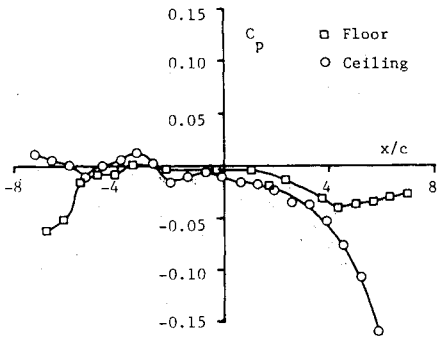

Fig. 8 Wind-tunnel static pressure distribution, model installed unswept, no-blowing, $\alpha = 0$ deg.

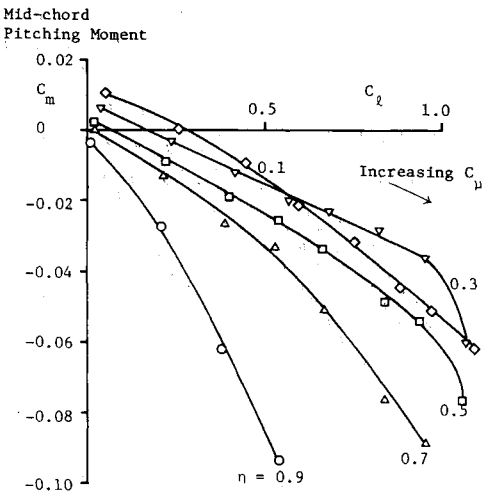

Fig. 9 Variation of lift coefficient with midchord pitching moment for the unswept configuration.

the actual blowing momentum coefficients between the two cases.

A difficulty encountered during this experiment, especially for the aft-swept configuration, was that the wind-tunnel working section exhibited a strong streamwise static pressure gradient in the vicinity of the model.

This gradient was not due to the presence of the model and is illustrated in Fig. 8. The first-order effect of this variation may be observed on the previously shown pressure distributions as a vertical shift of the pressure coefficients. The effect

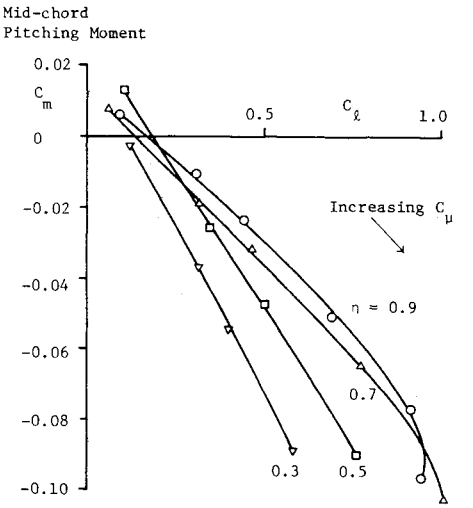

Fig. 10 Variation of lift coefficient with midchord pitching moment for the swept configuration.

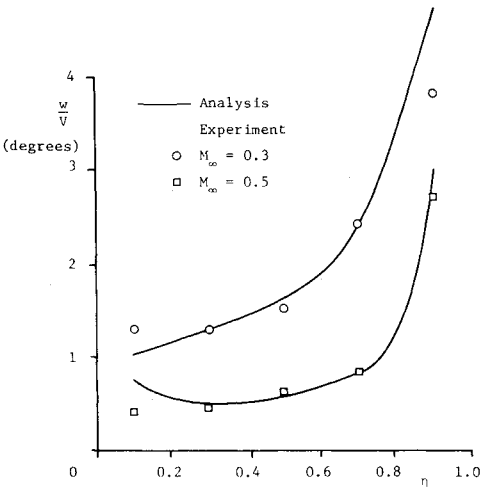

Fig. 11 Estimates of downwash distribution, unswept.

on the integrated overall lift and moment coefficients appears to be small. Also implied is a negative shift in the angle of the freestream relative to the tunnel walls, as indicated by the increasing pressure differences between the floor and ceiling distributions. The effects of this shift have not been isolated with respect to the pressure differences, and the differences should not detract from the overall quality of the data.

Recently, Wood and Rogers[5] have shown that the gradient of the lift to midchord pitching moment curve may be used to estimate the effective angle of attack of a two-dimensional circulation control airfoil. This property arises from the fact that the midchord pitching moment of a circulation control airfoil was shown to be decoupled from the lift coefficient due to blowing in two dimensions. Figures 9 and 10 show the measured variations of these two parameters for a variety of span locations for both the swept and unswept cases. If the gradient of the curves is proportional to the incidence correction, then it is apparent that the downwash distributions are reversed from the swept to the unswept case as previously suggested. It should of course be noted that these angular corrections include any lift interference due to the proximity of the tunnel boundaries. Wood and Rogers also showed that the two-dimensional lift interference for a circulation control airfoil is linearly proportional to the lift coefficient, the constant of proportionality being a function only of the airfoil chord/tunnel height ratio. The angular correction due to lift interference for this wind tunnel and a 10 in. chord airfoil has

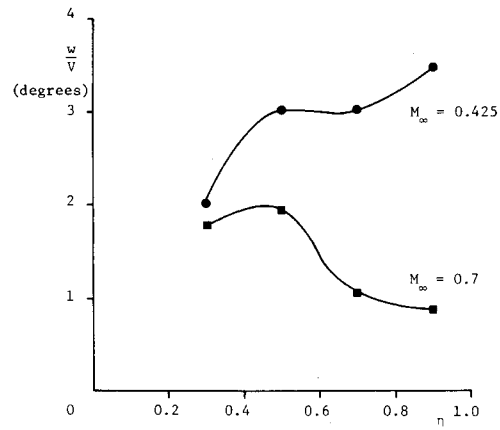

Fig. 12 Empirical estimate of downwash distribution for the swept configuration.

been approximated as

$$\Delta\alpha = -0.5C_\ell \text{ (deg)}$$

This value may then be used in a strip theory approximation, in conjunction with Figs. 9 and 10, to determine the local downwash angle along the span, assuming that the variation of the midchord pitching moment is known as a function of angle of attack. It was assumed that the variation of midchord pitching moment with effective angle of attack was zero and that the variation of the pitching moment with angle of attack was deduced from no-blowing alpha sweeps of the finite wing. Ideally, such data should be obtained from two-dimensional airfoil tests. This would permit absolute values of downwash to be determined as opposed to the relative values deduced in this work.

To justify this technique further, a simple series expansion method[6] was used to determine the downwash angle from a given load distribution, this method being applicable only to the unswept data. The load distribution is approximated by the following series expansion:

$$C_\ell = \frac{8s}{S}\sum_1^\infty A_n \sin(n\theta)$$

The coefficients of the expansion may be determined to satisfy as many known load points as required (in this case, 5), and the downwash may then be evaluated from the following equation:

$$\frac{w}{V} = \frac{\sum_1^\infty nA_n \sin(n\theta)}{\sin(\theta)} \quad \text{(deg)}$$

The results from this analysis are given as Fig. 11 for the unswept configuration. The agreement between the analytical and the empirical results for the unswept data is thought to adequately justify the extension of the empirical technique to the swept configuration. Notice the deviation between the techniques at the root and tip of the wing. It is suggested that this is a property of the finite nature of the blowing slot on the wing. At the ends of the jet, the jet sheet is "ripped" away from the Coanda surface to form an extremely intense vortex which, for the tip flow, was seen (by using a laser light sheet) to be shed parallel to the main wing-tip vortex with little or no interaction. It is of interest to note that at the tip, for a positive lift case, the signs of the vorticity are the same. However, for the case of a negatively loaded blade with positive lift due to blowing, a not uncommon occurrence in a rotary-wing environment, the shed vortices may be of opposite sign. The interaction of these two structures may produce some extremely complicated flowfields, which in turn are very

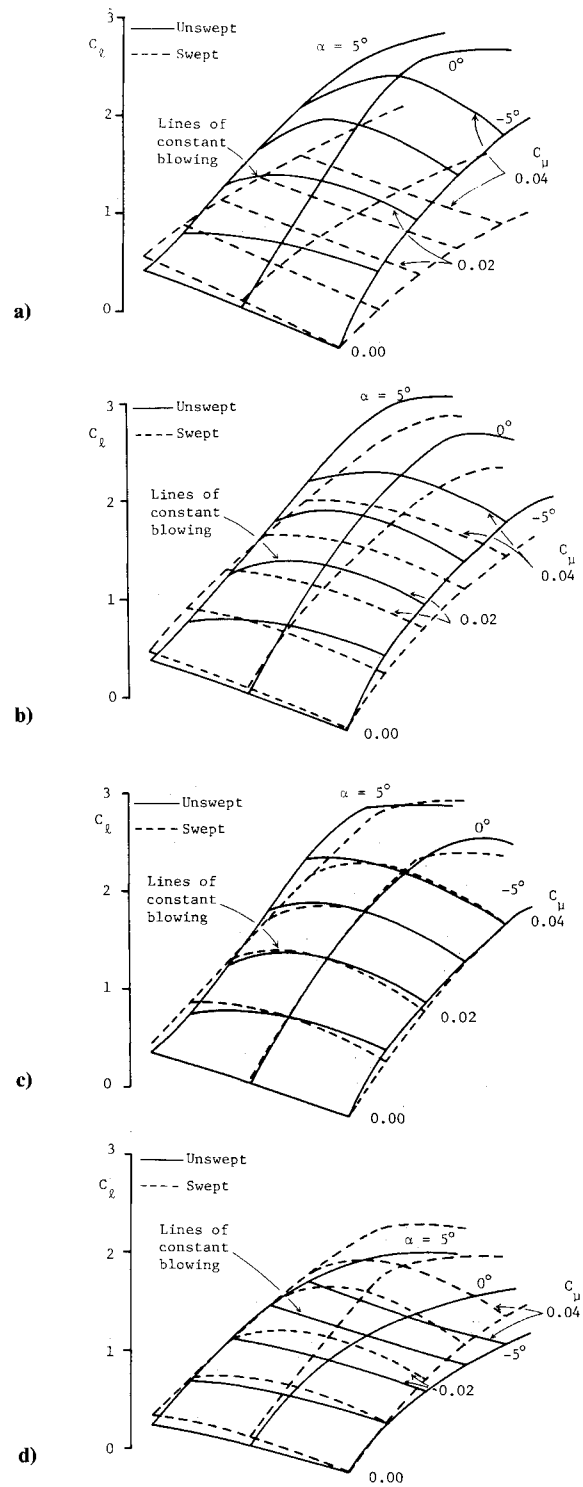

Fig. 13 Carpet plot of lift at a) $\eta=0.3$, b) $\eta=0.5$, c) $\eta=0.7$, and d) $\eta=0.9$.

time-dependent and periodic. A similar occurrence is anticipated at the root of the wing although the resulting flowfield will depend largely on the hub characteristics. The shedding of these additional intense vortices is suggested to account to some degree for the disagreement between the analytical and empirical downwash distributions in the unswept configuration and may be of significance in terms of wake prediction and blade/vortex interactions for rotating circulation control wings.

Figure 12 shows the results of the calculations to determine the downwash distributions for the swept configuration from the lift-pitching moment curves. It is immediately apparent

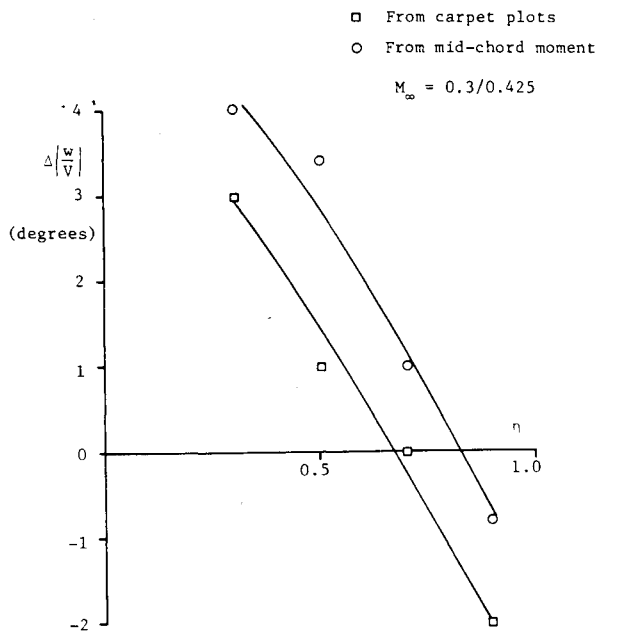

Fig. 14 Estimates of the change in downwash between the two configurations.

that the distributions are significantly different from those obtained for the unswept configuration. No simple analytical method exists to deduce the downwash due to a swept lifting wing, and therefore no comparison was attempted. Such a marked difference in the downwash distributions was anticipated to be a key factor in removing any finite wing effects to enable a comparison of the effects of sweep between the two configurations. A simple method for examining the interaction of the effects of wing sweep and three-dimensional flow is to compare the differences in the downwash distributions for the swept and unswept configurations from two separate methods. First, an estimate of the downwash may be deduced from the technique previously described using the midchord pitching moment. Second, an estimate of the difference in the downwash may be inferred from examination of carpet plots of the lift performance. Figure 13 shows carpet plots (plots with linearly displaced origins corresponding to fixed increments of angle of attack) of the lift generation for the different spanwise locations with both swept and unswept data provided. These plots allow direct estimation of the difference in the effective angle of attack at each location for constant blowing conditions (assuming that the sections are performing in a two-dimensional manner). A comparable change in angle of attack (assumed to be due to the change in downwash) has been calculated for the same freestream conditions using the empirical pitching moment technique. The suggestion is that if the observed changes in lift augmentation across the span could be shown to be accountable for by the change in downwash, then the corrections for the effects of sweep would also apply across the span. Figure 14 shows the result of this comparison. Clearly some degree of agreement has been achieved by the two different techniques, thus substantiating the suggestion that the effects of sweep observed initially at the 70% spanwise station are representative of an infinite yaw experiment, even in the presence of a finite wing. The inboard shift of the data from the carpet plots may be due either to the change in tunnel static pressure and flow angle as previously described or to the nonperfect tip form in the swept configuration. A tip that maintained alignment with the freestream would perhaps have been more appropriate but in turn would have produced a more complex model.

An effect of increasing Mach number was observed on the relative behavior of the lift generation at the tip of the wing. As the speed increased, the difference between the swept and unswept performance tended to reduce, suggesting that the change in downwash tended to zero. This effect was observed to spread inboard to 60% span at this highest Mach number examined. The cause of the phenomenon is still unde investigation.

Closer examination of the measured pressure distributions has suggested that there is little or no effect of sweep on the point at which jet stall occurs. For all cases examined, the stall occurred when the minimum pressure on the Coanda surface achieved a value of approximately 1.4 times c_p^* (the local sonic condition). While this value disagrees somewhat with previous correlations[7] (which were closer to 1.0 times c_p^*), the difference may be attributed to difference in slot height and Coanda radius distribution. The observation that the factor is approximately constant is, however, of value to future airfoil performance estimation. While the load distributions measured on the finite wing depend on the sweep angle, the point of inception of the jet stall appeared, in addition, to be dependent on the downwash distribution. A stall was often initiated where extreme negative downwash angles were deduced from the lift/midchord pitching moment relationship. Presumably, the extreme negative angles of attack produced such a high lift augmentation that the blowing momentum required to reach the maximum lift due to blowing prior to 1.4 times c_p^* was reduced locally. In all cases, the c_p^* stall ratio appeared to be maintained. Unswept, the trailing-edge suctions were observed to be most intense toward the tip of the wing while, for the swept case, a more uniform distribution was apparent. This difference may again be related to the varying downwash distributions for the two configurations and the figures showing the effect of angle of attack on lift performance. For more negative angle of attack, the boundary layer approaching the slot becomes increasingly thin due to the more favorable pressure gradients. This in turn permits improved boundary layer control, a higher suction at the trailing edge and, consequently, a premature onset of jet stall.

Conclusions

A three-dimensional wind tunnel test on a finite circulation control wing has been completed. For up to 45-deg aft sweep angle, the scaling laws for conventional airfoils appear to apply equally well to circulation control airfoils. No effects of sweep on the jet/boundary-layer interaction have been observed within the limits of the test matrix. The attainable levels of lift augmentation, the jet stall conditions, and the effects of Mach number and angle of attack appear to be consistent with two-dimensional results.

Simple empirical and analytical methods have been used to show that the individual effects of sweep and three-dimensionality can be isolated and identified. In this manner, the effects of wing sweep were correlated across the entire span of the wing. Therefore, *providing* that the downwash distribution is known, two-dimensional data bases may be used to *estimate* the load distributions of finite circulation control wings with or without aft sweep.

The additional vorticity shed at the finite ends of the jet would appear to be important in determining the local downwash field and may be of equivalent magnitude to the conventional tip vortex. The downwash distribution is also critical in determining which segment of the three-dimensional wing will first reach jet or alpha stall conditions. The flows at both the root and the tip were seen to be highly three-dimensional and to require further detailed examination. Particular attention should be given to the wall/body of revolution/wing interaction and to the effects of different wing-tip planforms/tip blowing configurations.

References

[1]Wood, N. J. and Nielsen, J., "Circulation Control Airfoils—Past, Present, Future," AIAA Paper 85-0204, Jan. 1985.

[2]Keener, E. R., Sanderfer, D. T., and Wood, N. J., "Experimental Pressure Distribution Studies for a Swept Three-Dimensional Circulation Control Wing," NASA CP2432, Nov. 1986.

[3]Spaid, F. W., "Experimental Boundary Layer Studies for a Swept Three-Dimensional Circulation Control Wing," NASA CP2432, Nov. 1986.

[4]Kuchemann, D., *The Aerodynamic Design of Aircraft,* 1st ed., Pergamon, Oxford, England, 1978, pp. 221–251.

[5]Wood, N. J. and Rogers, E. O., "An Estimation of the Wall Interference on a Two-Dimensional Circulation Control Airfoil," AIAA Paper 86-0738CP, 1986.

[6]Houghton, E. L. and Brock, A. E., *Aerodynamics for Engineering Students,* 2nd ed., Edward Arnold, London, 1972, pp. 354–358.

[7]Abramson, J. and Rogers, E. O., "High Speed Characteristics of Circulation Control Airfoils," AIAA Paper 83-0265, Jan. 1983.